Short X-ray pulses in a Laue-case crystal

Walter Graeff

Hamburger Synchrotronstrahlungslabor Hasylab at Deutsches Elektronensynchrotron DESY, Hamburg, Germany.
E-mail: walter.graeff@desy.de

The short X-ray pulses coming out of a SASE FEL (self-amplified stimulated-emission free-electron laser) have stimulated a closer inspection of the response of a crystal reflection to them. After a short collection of formulae taken from the dynamical theory of X-ray diffraction, the response to a δ-pulse reflected by a Laue-case monochromator crystal is investigated. In contrast to the already discussed Bragg-case monochromator, a two-dimensional analysis is required.

Keywords: free-electron lasers; X-ray optics; dynamical diffraction.

1. Introduction

The X-ray beam emerging from a free-electron laser (FEL) has a rather special time structure. The numbers given here are valid for the XFEL, which is part of the linear collider project TESLA currently being proposed by DESY (1997). A similar project pursuing these synchrotron radiation sources in the X-ray regime, sometimes called fourth-generation sources, is planned in Stanford, USA (SLAC, 1998).

At TESLA-XFEL, every 200 ms a bunch train is released over 1 ms that consists of 11 315 bunches of length 180 fs. These bunches are subdivided in turn into bursts of coherent radiation with an average length of 0.1 fs. The r.m.s. spot size at the exit of the sources is estimated to be of the order of 25 µm. Thus the X-rays are coherent within cells with a transverse diameter of 50–60 µm (2.35 × r.m.s. value) and a very thin longitudinal dimension of 0.03 µm. The r.m.s. angular divergence is roughly 1 µrad, so that, after several hundred metres, the transverse diameter of these cells is of the order of several hundred µm, whereas diffraction in a crystal takes place in a layer thickness called the extinction length, which is of the order of 10 µm.

The reflection of short X-ray pulses has been studied by several authors (Wark & He, 1994; Chukovski & Förster, 1995; Tomov *et al.*, 1998; Wark & Lee, 1999; Shastri *et al.*, 2001*a*,*b*). In this paper, the time-dependence of X-ray diffraction is considered by describing the input radiation as an integral over plane waves, then the results of the dynamical theory are used for steady-state plane waves, and finally the time-dependent output radiation is obtained by Fourier back-transform, thereby following the approach of Shastri *et al.* (2001*a*). Time-dependent fundamental equations such as the time-dependent Takagi–Taupin equations (Chukovski & Förster, 1995) are not used.

In the symmetric Bragg case all reflected waves are parallel when the incident waves are parallel. In contrast, the reflected waves in the symmetric Laue case are divergent, even if the incident waves are parallel. This is due to refraction as, in the symmetric Laue case, reflecting net planes and the crystal surface are perpendicular to each other.

2. Description of the calculation

Although the calculation approach has already been given by Shastri *et al.* (2001*a*,*b*), we recall the formulae for the sake of completeness and clarification.

An arbitrary scalar wave may be considered as an appropriate superposition of plane waves, as plane waves represent a complete set of orthogonal functions,

$$E_{\rm in}(\vec{r},t) = \int \mathrm{d}^3k \int \mathrm{d}\nu\, \tilde{E}(\vec{k},\nu)\exp(2\pi i\vec{k}\vec{r} - 2\pi i\nu t). \qquad (1)$$

This generalized description of a wave must fulfil the wave equation, which means that there must exist a dispersion relation $\nu = |\vec{k}|\cdot c$ in the medium, here a vacuum. In order to proceed from this general assumption, we have to restrict ourselves further. In view of the fact that the first crystals are several hundreds of metres downstream of the source, we may consider the incoming beam as planar. All incident components of the $\vec{k}$-vector are parallel to each other. Nevertheless, the treatment must be carried out in two dimensions because of refraction. We further restrict ourselves to incident waves whose amplitude does not depend on its position on a plane perpendicular to the beam direction (justified by the very large transverse dimension of the incident beam compared with the longitudinal dimension). Finally, we simulate the short pulse by a δ-function,

$$\begin{aligned} E_{\rm in}(\vec{r},t) &= E_0\delta\left(t - \frac{\vec{K}_0^0}{|\vec{K}_0^0|}\frac{\vec{r}}{c}\right) \\ &= E_0\int \mathrm{d}\nu \exp\left[2\pi i\nu\left(\frac{\vec{K}_0^0}{|\vec{K}_0^0|}\frac{\vec{r}}{c} - t\right)\right], \end{aligned} \qquad (2)$$

where $\vec{K}_0^0$ is chosen in such a way that it exactly fulfils the Bragg condition. If we want to know the output of a crystal reflection, we have to compute its effect in ν space for each plane wave, a task already solved by the dynamical theory, and transform the result back to the real space. We may take the steady-state solutions from the dynamical theory as we restricted ourselves to transversely unbound waves. Regions close to the boundary of the beam cannot be investigated this way. Also, cases where the density of photons is so high that a significant part of the reflecting atoms are ionized cannot be investigated this way as this would require time- and space-dependent Fourier coefficients. Fortunately, at least with unfocused beams, this is not the case.

The measurable output signal is proportional to the intensity, which is defined as the square modulus of the electric field, thus any phase factor (*e.g.* owing to a shift of the origin) cancels.

For practical calculations we include the relation between power flow and electric field because the output signal considered in this paper is given as the square modulus of the electric field E, whereas the output of a FEL undulator is often given as the peak power flow. The power flow S of an electromagnetic wave (energy per time per area) is related to the electric field (voltage per length) by

$$S = (\varepsilon_0/\mu_0)^{1/2}E^2, \qquad (3)$$

where the reciprocal value of the root is known as the vacuum impedance which, in practical units, is 377 Ω.

We choose for the symmetric Laue case a coordinate system (x, z), where the x-axis is parallel to the surface of the crystal and the z-axis points into the crystal (in the figures, to the left and to the bottom, respectively). The origin of the spatial coordinate system lies on the entrance surface. The incident wavevector has a negative x-component and a positive z-component. Consequently, the central reflected wavevector has the opposite x-component and the same z-component, where $k = |\vec{K}_0^0|$ denotes the length of the mean wavevector in a vacuum,

$$
\begin{aligned}
K^0_{0x} &= -k\sin\Theta,\\
K^0_{0z} &= k\cos\Theta,\\
K^0_{hx} &= k\sin\Theta,\\
K^0_{hz} &= k\cos\Theta.
\end{aligned}
\tag{4}
$$

Considering a quasi-monochromatic wave with mean wavenumber k, Snellius' law requires the tangential components of wavevectors at a boundary to be constant.

The reflected wavevector inside the crystal, starting on the so-called dispersion surface, is found by the intersection of the dispersion surface and the surface normal through the point of the wavevector outside the crystal. The reflected wave behind the crystal is again found by the surface normal of the back side (which is identical to that at the entrance surface with a plane parallel crystal). For clarity, only wavevectors outside the crystal are shown in Fig. 1. As usual in the dynamical theory, the end points of the wavevectors on the reciprocal lattice points are kept fixed, whereas the starting points move on a circle for constant length (circles are approximated by their tangents as $\Delta k/k$ is very small). It follows in our case with a wavevector length change Δk (see Fig. 1; we have to keep in mind that we are looking at the starting points of the k-vectors, hence positive changes of the k-vectors go towards the right or upwards in the figure, although the coordinate system is defined oppositely),

$$
\begin{aligned}
K_{0x} &= K^0_{0x} + \Delta K_{0x} = K^0_{0x} - \Delta k\sin\Theta,\\
K_{0z} &= K^0_{0z} + \Delta K_{0z} = K^0_{0z} + \Delta k\cos\Theta,\\
K_{hx} &= K^0_{hx} + \Delta K_{hx} = K^0_{hx} - \Delta k\sin\Theta,\\
K_{hz} &= K^0_{hz} + \Delta K_{hz} = K^0_{hz} + (\Delta k/\cos\Theta)(1+\sin^2\Theta).
\end{aligned}
\tag{5}
$$

The change in wavevector magnitude may be interpreted as a nominal change $\Delta\Theta_0 = \Theta - \Theta_B$ in the incident angle. By differentiating Bragg's law a positive Δk results in a negative $\Delta\Theta_B$,

$$
\Delta k = -k\cot\Theta\Delta\Theta_B. \tag{6}
$$

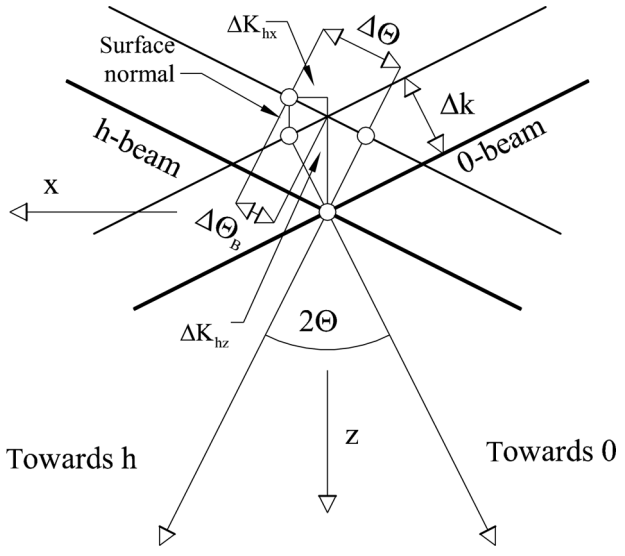

Figure 1
A change of the length of the incident wavevector Δk, but keeping its direction, causes a change in the reflected wavevector both in length and direction. The position of the reflected vector without changing its direction is also indicated. Note the difference between $\Delta\Theta$ and $\Delta\Theta_B$.

However, as we assume the incident angle to be constant, $\Delta\Theta_0 = -\Delta\Theta_B$ must hold, which means a change in the normalized incidence parameter,

$$
y = \frac{-\Delta\Theta_0\sin 2\Theta}{|\chi_h|} = -\frac{2\sin^2\Theta}{k|\chi_h|}\Delta k = -\frac{2\sin^2\Theta\Delta_e}{\cos\Theta}\frac{\Delta\nu}{c}, \tag{7}
$$

where

$$
\Delta_e = \cos\Theta/(k|\chi_h|), \tag{8}
$$

χ_h is the Fourier component of the dielectric susceptibility, usually complex to include absorption effects, and Δ_e is the Pendellösung length, in the Bragg case it becomes the extinction length. If y was a free parameter, it would also depend on $\Delta\Theta_B$ and $\Delta\nu$. In particular, $y = 0$ defines a plane symmetric to the reciprocal vectors $\vec{K}^0_0$ and $\vec{K}^0_h$. Negative values of y occur on the left-hand side of the symmetry plane and positive ones occur on the right-hand side (right and left with respect to Fig. 1). However, we are interested in a special manifold of y defined by the incident wave. Therefore, y depends on $\Delta\nu$ only.

$\Delta\Theta$ and $\Delta\Theta_B$ must not be confused. $\Delta\Theta$ measures the angular deviation of the reflected wavevector from a central $\vec{K}^0_h$ vector, whereas $\Delta\Theta_B$ measures the deviation from the centre of the reflection curve of a particular wavevector with magnitude $k + \Delta k$.

The amplitude of the reflected wave is now simply the sum of all corresponding plane waves with appropriate magnitude and phase, contained in $R(\nu)$. The dynamical theory has been treated by numerous authors in the past; for instance, in the article by Bonse & Graeff (1977) we find

$$
R(y) = i\varphi\left(\chi_h/\chi_{\bar{h}}\right)^{1/2}\exp(ia_hT + iAy)\,S(y,T), \tag{9}
$$

with the notation

$$
\begin{aligned}
\varphi &= \left(\chi_h\chi_{\bar{h}}\right)^{1/2}\Big/\left|\left(\chi_h\chi_{\bar{h}}\right)^{1/2}\right|,\\
a_h &= \pi k\chi_0/\cos\Theta,\\
A &= \pi T/\Delta_e,\\
S(y,T) &= \sin\left[A\left(y^2+\varphi^2\right)^{1/2}\right]\Big/\left(y^2+\varphi^2\right)^{1/2},
\end{aligned}
\tag{10}
$$

taking the origin at the entrance surface. T is the thickness of the crystal and A is the dimensionless thickness parameter used in the dynamical theory. Part of the abbreviations have a physical meaning: φ depends on the phase difference between the Fourier components χ_h and $\chi_{\bar{h}}$. For a centrosymmetric structure it is close to 1, if absorption is small. a_h describes refraction. $R(y)$ includes the generation of two wave fields inside the crystal and their interference at the back already. The necessary transformation from $R(y)$ to $R(\nu)$ can be made with the help of equation (7).

The general expression (1) is now formulated for our special case of an incident wave (2),

$$
E(x,z,t) = \int \mathrm{d}\nu R(\nu)\exp\left\{2\pi i\left[K_{hx}(\nu)x + K_{hz}(\nu)z - \nu t\right]\right\}. \tag{11}
$$

That there is no further weighting of the plane waves is due to the fact that we assume a δ-function in time as an incident wave where all plane waves are present in the spectrum with equal weight.

In order to facilitate the look-up of tabulated integrals we formulate the integral in terms of y. Extracting the central plane wave and the geometrical functions into a constant factor C, leaving only the differences, which are specified above, and expressing ν by y using (7), $K_{hx}(\nu)$ and $K_{hz}(\nu)$ by y using (5)–(7), the integral (11) becomes

$$E(x, z, t) = C \int \mathrm{d}y \exp(iAy)\, S(y, T) \exp\left\{\pi i\left[y \frac{\cos\Theta}{\Delta_e \sin^2\Theta} \times \left(x \sin\Theta - z \frac{1+\sin^2\Theta}{\cos\Theta} + ct\right)\right]\right\}. \quad (12)$$

We have to solve an integral of the form

$$\int \mathrm{d}y \exp(i\xi y)\, S(y, T), \quad (13)$$

which is formally the same task as solving the integral for an incident spherical wave, the result of which is well known, first obtained by Kato (1961*a*,*b*). In tables of Fourier transforms (*e.g.* Sneddon, 1951), we find the relation

$$(2\pi)^{-1/2} \int_{-\infty}^{\infty} \frac{\sin\left[b(a^2+x^2)^{1/2}\right]}{(a^2+x^2)^{1/2}} \exp(i\xi x)\, \mathrm{d}x = (\pi/2)^{1/2} J_0\left[a\left(b^2-\xi^2\right)^{1/2}\right], \quad (14)$$

where J_0 is the Bessel function of the zeroth order and $|\xi| < b$. Outside this range the integral vanishes. By making the following substitutions, $a \equiv \varphi$, $b \equiv A$, we can identify ξ to be

$$\xi \equiv A + \frac{\pi \cos\Theta}{\Delta_e \sin^2\Theta}\left(x \sin\Theta - z \frac{1+\sin^2\Theta}{\cos\Theta} + ct\right). \quad (15)$$

For convenience we set

$$\xi = A - (\pi/\Delta_e)\, z', \quad (16)$$

$$z' = \frac{\cos\Theta}{\sin^2\Theta}\left(-x \sin\Theta + z \frac{1+\sin^2\Theta}{\cos\Theta} - ct\right), \quad (17)$$

and obtain

$$J_0\left[\varphi\left(A^2-\xi^2\right)\right] = J_0\left\{\varphi(\pi/\Delta_e)[z'(2T-z')]^{1/2}\right\}. \quad (18)$$

Finally, the reflected amplitude is, again neglecting constants,

$$E(x, z, t) = J_0\left\{\varphi(\pi/\Delta_e)[z'(2T-z')]^{1/2}\right\}, \quad (19)$$

for $z > T$ and $0 \le z' \le 2T$.

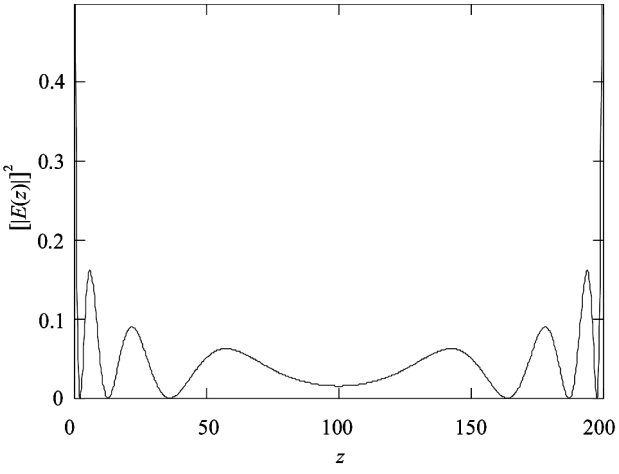

Figure 2
The intensity profile of the reflected wave just behind the crystal when the incoming pulse leaves the crystal. The vertical axis would extend to 1, but is truncated to enhance the central region. The horizontal axis is the parameter z' which runs from 0 to 200 μm, whereas the real coordinate x runs from 25.08 to 25.08 μm. Parameters used for the calculation: diamond 111 reflection, wavelength = 1 Å, crystal thickness T = 100 μm; see text for details.

3. Results and discussion

Let us now inspect the characteristics of the intensity distribution. The Bessel function is constant at a fixed time t for any combination (x, z), where x and z form straight lines, which are parallel to

$$z = \left[(\sin\Theta\cos\Theta)/\left(1+\sin^2\Theta\right)\right] x. \quad (20)$$

Note that these lines have a positive inclination. They run from the lower left to the upper right corner, whereas the planes perpendicular to the reflected wavevector, normally expected to contain the wave front, run from the upper left to the lower right corner.

An incident pulse which crosses the origin O at $t = 0$ has traversed the crystal after a time

$$t = \tau = T/c\cos\Theta. \quad (21)$$

The distribution of the reflected wave at the time τ just behind the crystal ($z = T$) is

$$E(x, T, \tau) = J_0\left[\varphi(\pi/\Delta_e)\left(T^2 - x^2\cot^2\Theta\right)^{1/2}\right], \quad (22)$$

shown in Fig. 2. The well known Pendellösung fringes structure may be seen, already known from an incident spherical wave, especially the strong spikes at the edges, known as the 'hot margins'.

For the same time τ [see equation (21)], intensity occurs along lines, the inclination of which is given by (20). A snapshot of the intensity is shown in Fig. 3. Only the reflected intensity is shown, the forward-reflected intensity is omitted. As a guide to the eye, the present position of the incident pulse is also indicated. As the image extends to infinity, it looks very similar for all times. A shift in time is simply a shift of the tip of the intensity distribution along the surface to the right.

The reflected intensity is confined to two limiting parallel lines, which means that no (longitudinal) broadening occurs when the reflected wave travels outside the crystal, as is normal in a non-dispersive medium.

Two findings are quite unusual: (i) the lines of constant intensity, as seen by the snapshot, are no longer perpendicular to the $\vec{K}$-vector; (ii) the intensity confined to two limiting lines requires that, after a certain characteristic time, which will be given below, each atom in the crystal stops to oscillate after the complete passage of the incident

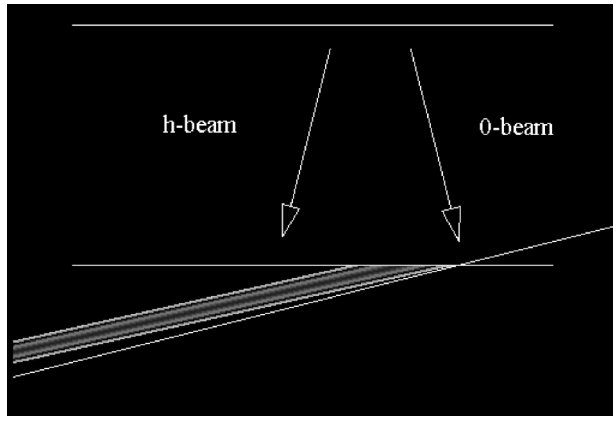

Figure 3
Snapshot of reflected and incident beams for a fixed time (white indicates high intensity). Note that the inclined line which represents the incident pulse travels in the 0-direction whereas the fringe structure travels in the h-direction. Also indicated are the boundaries of the crystal; values are the same as those given in Fig. 2.

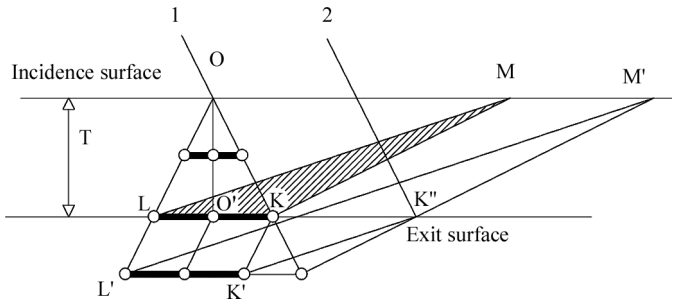

Figure 4
Physical interpretation of the result (see text).

pulse. This is in contrast to the Bragg case where, after the passage of a short pulse, there is always, at least theoretically, some energy left in oscillating atoms inside the crystal (see Shastri *et al.*, 2001*a*,*b*).

An observer at a fixed position behind the crystal will see the intensity in a time interval that is easily calculated from (17), recalling that z' is restricted to the interval $[0, 2T]$,

$$\Delta t = 2T \sin^2 \Theta/(c \cos \Theta), \tag{23}$$

a result already found by Shastri *et al.* (2001*a*). However, their treatment did not involve the refractive effects in Laue geometry.

In Fig. 4 we try to give a physical interpretation of the result. Consider the incident pulse, although infinitely wide in the transverse direction, to be composed of many pencil beams. Two of them are drawn in Fig. 4, namely 1 (pulse arriving at entrance) and 2 (pulse arriving at exit). The intensity distribution of pencil beam 1 is shown at three different times. When the pencil beam 1 hits the surface of the crystal it excites, as usual, two wavefields with slightly different k-vectors inside, which travel in all directions within the Borrmann triangle OKL. Assume the intensity distribution of the wavefields to be a δ pulse too. Circles indicate the pulse position in the margins (OL and OK) and in the centre (OO') at the different times. These reflected δ pulses lie again on straight lines as the group velocity of these wavefields depends strongly on their direction. For instance, in the centre of the reflection the wavefields travel parallel to the net planes and have a much lower group velocity than those travelling in the margins. This can be seen by recalling that the group velocity is given by $\mathrm{d}\nu/\mathrm{d}k$. In the centre of the reflection the dispersion is no longer determined by the circles around the reciprocal lattice points but by their intersection. This intersection point moves faster than the circles themselves, and the 'density' of dispersion surfaces in the centre is lower with changing k-value. Thus, the group velocity at the centre is $c \cos \Theta$ and all wavefields within the Borrmann triangle reach the exit surface at the same time. There, the local wavefields decompose and, according to their relative phase, form the well known Pendellösung pattern. At that moment the triangle KLM is filled with oscillating atoms only. Behind the crystal the reflected intensity travels along $\vec{K}_h$ and the tip of the intensity distribution of the whole pulse moves to the right (M to M' inside the crystal and K to K'' behind).

In order to provide some practical numbers, we consider a particular reflection, namely the 111 reflection from a diamond crystal, wavelength $\lambda = 1$ Å, because this reflection is that most likely to be used for further monochromatization of the output radiation of a FEL undulator.

Numerical values of the Fourier coefficients are (Stepanov, 2001)

$$\begin{aligned} \chi_0 &= -9.56 \times 10^{-6} + i(5.0 \times 10^{-9}), \\ \chi_h &= -3.47 \times 10^{-6} + i(3.5 \times 10^{-9}). \end{aligned} \tag{24}$$

The Bragg angle is $\Theta = 14.08^\circ$. Half of the Pendellösung length Δ_e in the symmetric Laue case is 27.95 µm. The time interval when intensity is present in the reflected beam with a 100 µm-thick diamond crystal amounts to $\Delta t = 40.7$ fs.

By making the crystal thinner and thinner, one could make the pulse width narrower and narrower. The integrated reflectivity with varying thickness starts from zero (kinematic region) and oscillates around an average value owing to the Pendellösung effect (see, for example, Pinsker, 1978). The maximum reflectivity is reached at $A = 1.22$ which, for the reflection above, corresponds to $T = 10.9$ µm and $\Delta t = 4.4$ fs. This time resolution is comparable with the Bragg case but still shows the double structure. Making such a thin crystal is certainly a technical challenge but would help a lot with the heat load that a monochromator must cope with in an XFEL beam. As one of the referees pointed out, the sample in timing experiments should be tilted in such a way that the reflected beam arrives at the same time on the sample surface.

The author is very grateful to C. Malgrange, G. Materlik and H. Schulte-Schrepping for elucidating and helpful discussions.

References

Bonse, U. & Graeff, W. (1977). *X-ray and Neutron Interferometry* in *Topics of Applied Physics*, Vol. 22, edited by H.-J. Queisser, pp. 93–143. Berlin: Springer.
Chukovski, F. N. & Förster, E. (1995). *Acta Cryst.* A**51**, 668–672.
DESY (1997). DESY report 1997-048, ECFA 1997-182. Deutsches Elektronensynchrotron DESY, Hamburg, Germany.
Kato, N. (1961*a*). *Acta Cryst.* **14**, 526–532.
Kato, N. (1961*b*). *Acta Cryst.* **14**, 627–635.
Pinsker, Z. G. (1978). *Dynamical Scattering of X-rays in Crystals*, p. 65, p. 490. Berlin/Heidelberg/New York: Springer-Verlag.
Shastri, S. D., Zambianchi, P. & Mills, D. M. (2001*a*). *Proc. SPIE*, **4143**, 69–77.
Shastri, S. D., Zambianchi, P. & Mills, D. M. (2001*b*). *J. Synchrotron Rad.* **8**, 1131–1135.
SLAC (1998). Report SLAC-R-521, UC-414(1998). Stanford Linear Accelerator Center, CA 94025, USA.
Sneddon, I. N. (1951). *Fourier Transforms*, p. 523. New York: McGraw-Hill.
Stepanov, S. (2001). χ_{0h} *on the Web*, http://sergey.bio.aps.anl.gov/.
Tomov, I. V., Chen, P. & Rentzepis, P. M. (1998). *J. Appl. Phys.* **83**, 5546–5548.
Wark, J. S. & He, H. (1994). *Laser Part. Beams*, **12**, 507–513.
Wark, J. S. & Lee, R. W. (1999). *J. Appl. Cryst.* **32**, 692–703.

Received 20 August 2001 • Accepted 30 January 2002